Renewable and Sustainable Energy Reviews 35 (2014) 31–41

Contents lists available at ScienceDirect

Renewable and Sustainable Energy Reviews

journal homepage: www.elsevier.com/locate/rser

Assessment of the greenhouse climate with a new packed-bed solar air heater at night, in Tunisia

Salwa Bouadila*, Mariem Lazaar, Safa Skouri, Sami Kooli, Abdelhamid Farhat

Research and Technology Center of Energy, Thermal Processes Laboratory, Hammam Lif, B.P. 95, 2050 Tunis, Tunisia

ARTICLE INFO

Article history:
Received 26 May 2013
Received in revised form
26 February 2014
Accepted 21 March 2014
Available online 15 April 2014

Keywords:
Latent heat storage
Packed bed solar air heaters
Control climate greenhouse

ABSTRACT

The use of solar energy for heating greenhouses in the cold period for a Mediterranean climate is an important issue. In this paper, the thermal performance of a new solar air heater using a packed bed of spherical capsules with the latent heat storage system in east–west oriented greenhouse, is analyzed and discussed. The excess heat in the greenhouse was stored in the packed bed through the diurnal period and extracted at night. An experimental comparative study was conducted in two greenhouses installed in the Research and Technologies Centre of Energy (CRTEn) in Tunisia. The greenhouse heat balance in different components of the greenhouse with a heating system (cover, canopy, soil, inside air and packed bed solar collector), has been used to investigate the impact of the phase change material (PCM) on the greenhouse temperature and humidity. Results show that the nocturnal temperature inside the greenhouse equipped by a heating system exceeds the temperature inside the conventional greenhouse by 5 °C. The relative humidity was found to be of an average 10–20% lower at night time inside the heated greenhouse. The nighttime recovered heat of the solar system attained 31% of the total requirements of heating. An economic evaluation was made to find the payback period of the new solar air heater, the potential in saving fuel energy and the reducing carbon dioxide emissions.

Contents

* Corresponding author. Tel.: +216 7143 0044/71 430 215; fax: +216 7143 0934.
E-mail addresses: salwa.bouadila@crten.rnrt.tn, bouadilasalwa@yahoo.fr (S. Bouadila).

http://dx.doi.org/10.1016/j.rser.2014.03.051
1364-0321/

1. Introduction

Greenhouses have been used in various forms of protection for the plants when it would have been impossible to grow outside because of the adverse climate, diseases and pests. The greenhouse permits to achieve maximum returns from cultivation by creating better growing conditions. The growth factors namely light, humidity, temperature and nutrition should be delivered and maintained at optimal levels [1,2]. To keep the optimum growing environment, greenhouses should allow high light transmittance, sufficient ventilation efficiency, low construction costs and low heat consumption [1,3]. With the present increase in the cost of fossil fuels, alternate energy sources may help to increase the profitability of greenhouses and the income of farmers [4]. The basic strategy of the greenhouse passive heating system is to reduce the heat losses while transferring the excess heat from inside the greenhouse during the day to heat storage. This heat is used during the night to satisfy the heating needs of the greenhouse [5,6].

Alternate sources of energy like solar energy have been proposed for heating greenhouses and providing the optimum inside conditions during winter months. Solar energy is a universally available source, but its practical use still presents some technical, and most importantly, economic problems [7]. Some solar systems have been developed but they are too expensive for commercial use [7]. Several types of passive solar systems and techniques have been proposed and used by [8–11]. Bargach et al. [10] used a solar fat-plate collector to improve the internal greenhouse microclimate and tested it under two types of days; a clear day and a cloudy one. Du et al. [12] developed a model to predict the performance of the greenhouse that is heated with a heat-pipe system. The model is validated with experimental data.

Thermal energy can be stored as sensible heat, latent heat, reaction heat or combination of those forms. Many thermal energy storage systems and applications are cited in literature [13–17]. The most important existing greenhouse heating systems that use a sensible stored energy are: water storage [18], rock bed storage [19,20] and ground storage [21,22]. The latent thermal storage has many advantages over the sensible one such as: high heat capacity, less volume, low storage temperature, thermal energy stored and released at an almost constant temperature. There is a large number of Phase Change Materials (PCMs) that melt and solidify at a wide range of temperatures which are used in greenhouse, such as $CaCl_2 \cdot 6H_2O$, $Na_2SO_4 \cdot 10H_2O$ and paraffin [23–27]. Kern and Aldrich [28] utilized a $CaC1_2 \cdot 6H_2O$ in aerosol cans that was used to investigate energy storage possibilities both inside and outside a 36 m^2 ground area of the greenhouse. The energy storage unit inside the greenhouse (contained 1650 kg PCM) absorbed the excess energy of warm air inside the greenhouse during the daytime. The energy storage unit outside the greenhouse contained 1376.4 kg PCM and two solar air collectors with 8.55 m^2 surface area each. Results of this study showed that, the energy stored by the outside unit was between 105.5 and 158.25 MJ, these were, 21.1 and 31.65 MJ for the internal unit. Huang and Toksoy [29] placed 3000 kg of $CaCl_2 \cdot 6H_2O$ in the heat exchanger inside a 200 m^2 glass covered greenhouse, and found that the interior air temperature was maintained at 2 °C higher than the outdoor conditions. Levav and Zamir [30] used $CaCl_2 \cdot 6H_2O$ in greenhouses and reported that the required air temperature in the greenhouse was achieved without any increase in the relative humidity. Boulard and Baille [31] utilized, in a greenhouse with 176 m^2 ground areas, double polycarbonate-cover and forced ventilation, 2970 kg of $CaCl_26\ H_2O$. The PCM was packed in containers and placed along the north wall. The PCM could provide 30% night heating needs during the winter period. Boulard et al. [32] used a $CaCl_2 \cdot 6H_2O$ latent heat storage system in a double-skin polycarbonate greenhouse equipped with a forced ventilation system. They found the inside greenhouse temperature roughly 10 °C higher than the outside temperature during typical nights of March and April. Ozturk et al. [33] performed an experimental evaluation of energy and exergy efficiency of a seasonal latent heat storage system for greenhouse heating using 6000 kg of paraffin wax as a PCM in a 180 m^2 greenhouse ground areas. They observed that the average energy and exergy efficiency of the arrangement was 40.4% and 4.2%, respectively.

The aim of this work is to determine the provided heat by a Solar Air Heater with Latent Storage Collector (SAHLSC) inside an Insulated Greenhouse with Latent Heat System (IGLHS). Experiments were carried out in two greenhouses designed and realized in the Research and Technology Center of Energy (CRTEn) in Tunisia. We will present in Section 2, the potential of solar energy in Tunisia. In Section 3, we will describe the design of the experimental greenhouses, the experimental setup and measuring equipments. In Sections 4 and 5, a thermal analysis of the climate greenhouse and the energy balance of the SAHLSC are carried out. The thermal load leveling (TLL) are defined in Section 6. The experimental results are reported in the Section 7. Finally, we will present the economic analysis of the SAHLSC in Section 8. The main remarks of this work will be reported in the conclusion.

2. Potential of solar energy in Tunisia

The average amount of solar energy radiating in Africa is about 6 kWh/m^2/day, depending on the latitude of the country [34]. In the map of average global horizontal solar radiation (Fig. 1), we can see that there's an important solar potential in North-Africa.

Tunisia is one of the sunlight countries, it lies on the Mediterranean coast of Africa; it is bordered by Algeria to the west and Libya to the southeast; with the following coordinates: Latitude 36°43′N and Longitude 10°25′E. Tunisia's climate is temperate in the north, with mild rainy winters and hot summers. Temperatures in July and August can exceed 40 °C, while winters are mild with temperatures rarely exceeding above 20 °C [35].

The meteorological station on the site of Borj Cedria in Tunisia permits the measurement of the global sun flux on a horizontal plan, ambient temperature, wind speed and wind direction. Figs. 2 and 3 give the variation of meteorological data of the average monthly global solar radiation and ambient temperatures in a period of 2009–2011. We can see that the global solar flux has the same trend of variation as the ambient temperature. It is observed that the peak of average monthly radiation is registered in July (225 kW/m^2) with a highest monthly ambient temperature surrounding 30 °C. The least average monthly radiation is 65 kW/m^2 with a monthly ambient temperature around 13 °C in December.

Nomenclature

A	surface area (m^2)
C_p	specific heat of air at constant pressure (J/kgK)
d_a	density of air (kg/m^3)
H	heat loss coefficient of SAHLSC (W/m^2°C)
h	heat transfer coefficient (W/m^2 °C)
I_T	total solar radiation (W/m^2)
L	latent heat (J/kg)
LAI	leaf area index
L_{gh}	characteristic length of greenhouse (m)
L_1	collector length (m)
L_2	collector width (m)
L_3	collector depth (m)
l	characteristic length of the leaf canopy (m)
l_{ca}	average length of the canopy (m)
m	mass (kg)
$\dot{m}$	mass flow rate (kg/s)
Nu	Nusselt number
$P(T)$	saturated water vapor pressure at temperature T (kPa)
Pr	Prandtl number
Q	heat rate (W)
Ra	Rayleigh number
RE	rate of air infiltration (m^3/s)
Re	Reynolds number
r_a	aerodynamic resistance (s/m)
r_s	stomatal resistance (s/m)
T	temperature (K)
t	time (s)
U	velocity (m/s)
V	volume (m^3)
z	depth of soil (m)

Greek symbols

α	absorbtivity for solar radiations
α_t	absorbtivity for thermal radiations
δ_b	bottom insulation thickness (m)
δ_e	edge insulation thickness (m)
Δ	difference in time
ε	emissivity
γ	psychometric constant, 0.0667 kPa/K
λ	thermal conductivity (W/m K)
λ_i	thermal conductivity of insulation (W/m K)
μ	PCM dynamic viscosity (Ns/m^2)
μ_s	PCM dynamic viscosity at $T = T_{PCM}$ (Ns/m^2)
ρ	reflectivity
σ	Stefan–Boltzmann constant, 5.670×10^{-8} W/m^2 K^4
τ	transmissivity

Subscripts

A	absorbed
a	ambient
av	average
c	cover of greenhouse
ca	canopy
b	bottom
ch	charging
dis	discharging
e	edge
fin_ch	final of the charging process
fin_dis	final of the discharging process
g	glasses of SAHLSC
H	heat gain
i	inside greenhouse
in	inlet of SAHLSC
inf	infiltration
L	liquid phase
los	leakage, losses
m	melting
max	maximum
min	minimum
o	outsider greenhouse
out	outlet of SAHLSC
PCM	phase change material
p	packed-bed absorber
S	solid phase
s	soil
sky	sky
st	storage
t	top
u	useful
v	vertical section of the greenhouse

Exposants

A	absorbed heat
C	convective heat
Cd	conductive heat
L	latent heat
R	radiation heat

3. Materials and methods

3.1. Experimental greenhouses description

In this study, experiments were carried out in two small chapel-shaped greenhouses with same dimensions. The experimental greenhouses occupy a floor area equal to 14.8 m^2, 3.7 m wide, 4 m long and 3 m high at the center. The structure is all galvanized steel fixed to the ground with stones and concrete. The greenhouses are equipped with a centrifugal fan controlled by a differential thermostat. The fan operated when the temperature inside the greenhouse exceeds the optimal growth temperature of plant. A tomato crop (local variety) was planted in both greenhouses and planted at 7 plants in the row and arranged in 4 rows with 40 cm between the rows and 35 cm between the plants.

Physical characteristics of the greenhouse glass cover, canopy and soil are listed in Table 1. The reflectivity and transmissivity spectra of the canopy and cover layer recorded in the wavelength range (380–1400 nm) were plotted in Figs. 4 and 5. respectively. The reflectivity and transmissivity spectra were realized using LAMBDA950 UV–vis–NIR spectrometer equipped with an integrating sphere.

The first greenhouse is named a Conventional Greenhouse (CG) where its walls and roofs are covered with a 3 mm of thick glass (Fig. 6). The second used a heating system and was named as an Insulated Greenhouse with Latent Heat System (IGLHS) (Fig. 7(a)). The south oriented wall and roof of the IGLHS are covered with a 3 mm of thick glass. Sidewalls and the northern roof are built with 0.4 m and 0.6 m of thick sandwich panels respectively.

The heating system of the IGLHS is a new Solar Air Heater with Latent Heat Storage Collector (SAHLSC) using a packed bed of

spherical capsules as a latent heat storage system [36]. A new type of the SAHLSC was designed as a means to heat the interior environment of the greenhouses during the nighttime. Fig. 7 (b) shows the SAHLSC manufactured inside the IGLHS. The length, the width and the total volume of the collector are 2 m, 1 m and 0.28 m^3, respectively. A 0.004 m of thick transparent glass cover was placed 0.015 m apart from the packed bed absorber. A 0.05 m thick polyurethane insulation, with heat conductivity of 0.028 $Wm^{-1} K^{-1}$, is placed in the bottom and the edge of the collector. The packed bed absorber is the most important component of the solar air heater collector, formed of spherical capsules with a black coating and fixed with steel matrix. Capsules, confined with a PCM, have an outer diameter of 0.077 m and are blow molded from a blend of polyolefin with an average thickness of 0.002 m [36].

3.2. Experimental setup and measuring equipments

Experimental greenhouses (east–west orientation), are constructed and located in the Research and Technology Center of Energy in Borj Cédria, in Tunisia.

During the sunshine time (charging process) a fraction of the total solar radiation received inside the greenhouse is absorbed by the black packed bed absorber surface of the SAHLSC. The absorbed thermal energy is stored as a sensible and a latent heat forms into the collector. At night, a fan blows air across the PCM capsules and extracted the stored heat into the IGLHS, the discharging process done.

K-type thermocouples inserted inside and outside the greenhouses for measuring the horizontal distributions of temperature, the vertical

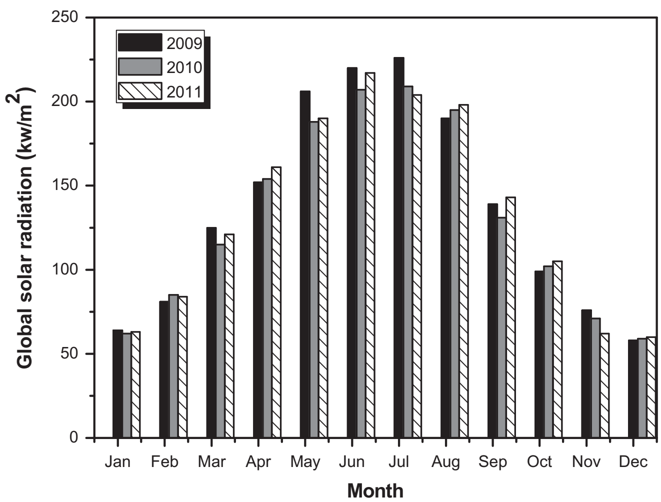


Fig. 2. Monthly variation of the global solar radiation in Tunisia (2009–2011).

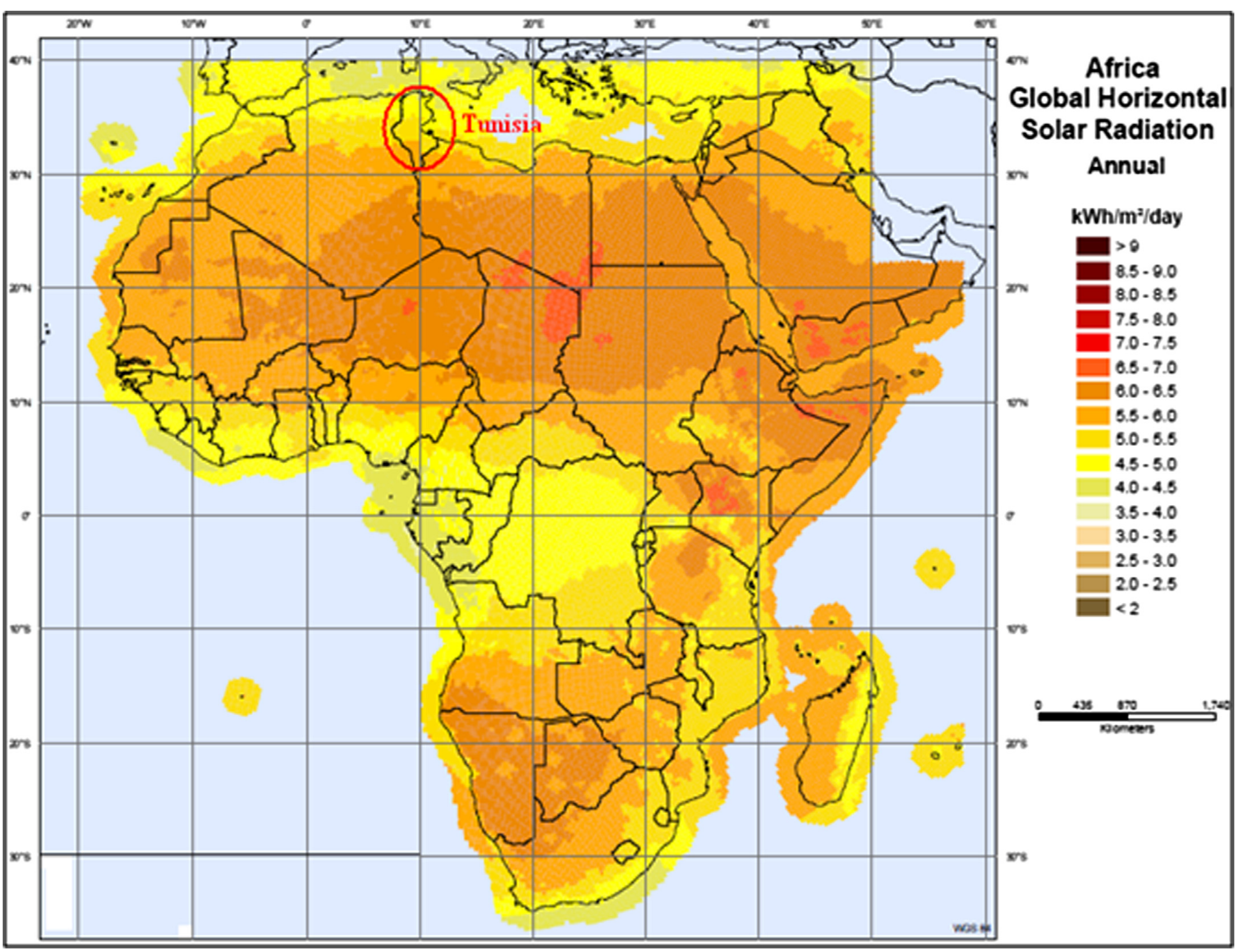


Fig. 1. Global solar radiation map of Africa [34].

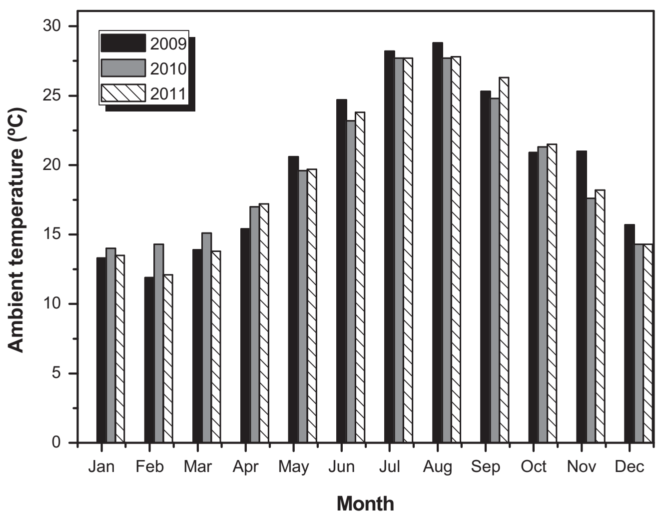


Fig. 3. Monthly variation of the ambient temperature in Tunisia (2009–2011).

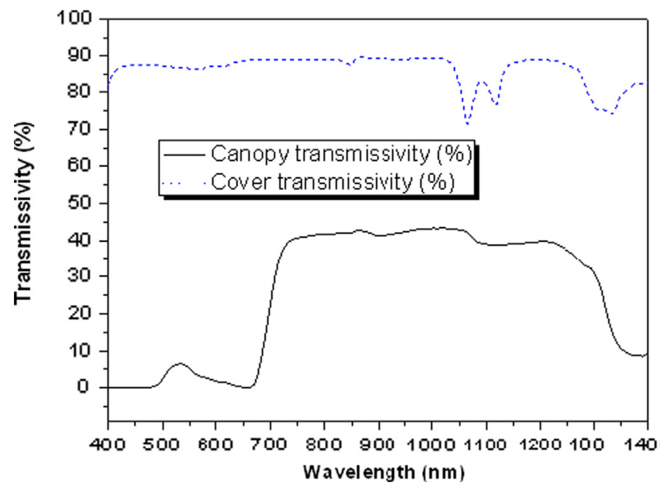


Fig. 5. Transmissivity spectra of canopy and cover.

Table 1
Cover, canopy and soil characteristic.

	Cover	Canopy	Soil
Reflectivity for solar radiations	0.10	0.1	0.2
Reflectivity for thermal radiations	0.10	0.55	0.16
Emissivity	0.9	0.95	0.9
Transmissivity for solar radiations	0.85	0	0
Transmissivity for thermal radiations	0.88	0.4	0



Fig. 6. External view of conventional greenhouse.

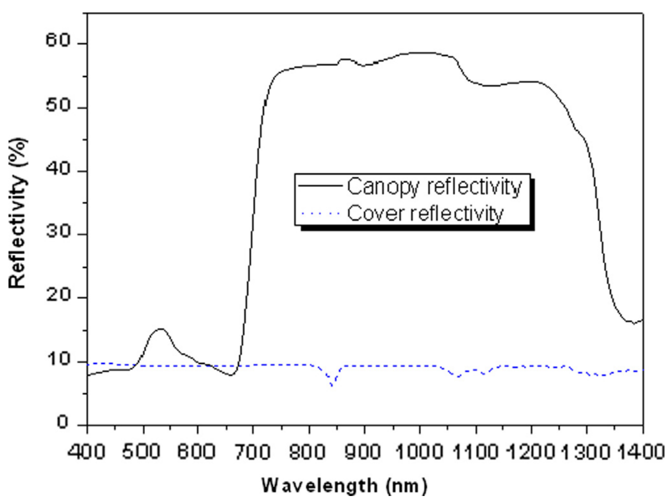


Fig. 4. Reflectivity spectra of canopy and cover.

distributions and the temperatures at the top and the bottom of glass and sandwich panel. The temperature and relative humidity inside greenhouses (HMP155A, Campbell Scientific Inc) were measured in the center at a height of 1.5 m from the ground. The HMP155A sensor was instaled inside a 14-plate radiation shield houses and protects. Its louvered construction allows air to pass freely through the shield, thereby keeping the probe near ambient temperature [37]. Temperatures under the soil inside the greenhouse at 0, 0.25 and 0.5 m depth were measured using three PT-107 sensors. The average temperature of the canopy was measured using a non-contact means of measuring the surface temperature by an infrared temperature sensor IR120. The IR-SS Solar Shield is used to protect the IR120 sensor from direct solar radiation [37]. The global solar irradiation in the horizontal plane was measured with a Kipp and Zonen pyranometer and situated at 1.5 m above the ground in the center of the IGLHS. Ambient temperature and relative humidity are measured by a HMP155A sensor situated at a height of 1.5 m above the greenhouse. Temperatures along the SAHLSC were measured using K-type thermocouples. Four sensors were inserted inside the capsules along with the absorber packed bed. Also four thermocouples are used to measure the absorber surface of one capsule, the glass, the inlet and the outlet air temperatures of the SAHLSC. All climatic parameters and measuring instruments were sample recorded every 10 min using a CR5000 data logger (Campbell Scientific Inc).

The external global solar radiation, wind speed and direction are provided by the NRG weather station in the Research and Technology Center of Energy in Tunisia. This station is equipped with an acquisition system that record, every 10 min the average, the maximum, the minimum and the standard deviation values for each sensor. The weather station provided a wind speed measurement at 20 m. The wind velocity at the altitude of 2 m above the greenhouse was corrected by using the power law equation [38]

$$(U_1/U_2) = (h_1/h_2)^{\beta} \quad (1)$$

where U_1 and U_2 are the wind speeds at heights h_1 and h_2 respectively. β is the power law exponent and the subscripts (1 and 2) correspond to different heights.

Uncertainty analysis is needed to prove the accuracy of the experiments. The independent parameters measured in the experiments reported here to temperature, air velocity, and solar

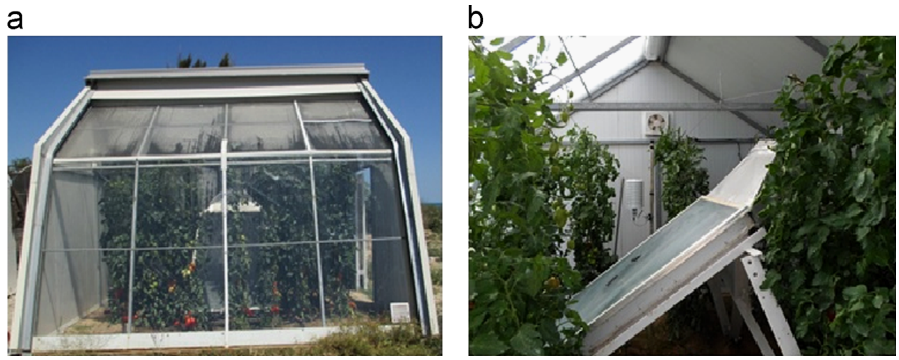


Fig. 7. (a) External view of IGLHS and (b) SAHLSC inside greenhouse.

radiation. To carry out these experiments, the sensitiveness of data acquisition system is about ± 0.001 °C, the measurement error is ± 0.002 °C, the sensitiveness of the thermocouple is ± 0.01 °C, the sensitiveness of the IR120 is ± 0.0004 °C and sensitiveness of the PT107 is ± 0.01 °C. The HMP155A errors are ± 0.02 °C about temperature and $\pm 2\%$ about humidity. An anemometer with $\pm 0.01\ ms^{-1}$ accuracy, and Kipp and Zonen pyranometer with $\pm 3\%$ measurements uncertainties were used. The sensitiveness was obtained from a catalog of the instruments.

4. Thermal analysis of greenhouse

To describe the thermal behavior of the greenhouse, there are four components that play important roles in the thermal balance: the cover, the canopy, the soil and the inside air are analyzed. The following assumptions are made:

- Radiation heat exchange between the greenhouse walls and roofs is neglected.
- Storage capacity of the sandwich panel walls and roof material is neglected.
- Absorbtivity and heat capacity of the enclosed air is neglected.
- Conduction heat exchange between air and the sandwich panel walls and roof of the greenhouse is neglected.

4.1. Energy balance of greenhouse cover

The energy balance of the cover of greenhouse described by the following equation:

$$Q_c^A + Q_{ca-c}^A + Q_{s-c}^A - Q_{c-o}^C - Q_{c-i}^C + Q_{c-sky}^R + Q_{s-c}^R + Q_{ca-c}^R = 0 \tag{2}$$

where Q_c^A is the solar radiations absorbed by the glasses of the greenhouse; Q_{ca-c}^A is the solar radiations reflected by the canopy and absorbed by cover; Q_{s-c}^A is the reflected solar radiations by the soil surface and absorbed by cover; Q_{c-o}^C is the convective heat transfer from external cover of the greenhouse to ambient air; Q_{c-i}^C is the convective heat transfer from internal cover of the greenhouse to inside air; Q_{c-sky}^R is the thermal radiation exchanged between cover and sky; Q_{s-c}^R is the thermal radiation emitted by soil surface and absorbed by cover and Q_{ca-c}^R is the thermal radiation emitted by canopy and absorbed by cover.

The energy balance of the cover Eq. (2) can be written as

$$I_T A_c \alpha_c + I_T \tau_c \alpha_c \rho_{ca} A_{ca} + I_T \tau_c \alpha_c \rho_s A_s - h_{c-o}^C A_c (T_c - T_o) - h_{c-i}^C A_c (T_c - T_i) + \sigma \varepsilon_c A_c (T_{sky}^4 - T_c^4) + A_s \sigma \alpha_{t,c} \varepsilon_s {T_s}^4 + A_{ca} \sigma \alpha_{t,c} \varepsilon_{ca} T_{ca}^4 = 0 \tag{3}$$

Different relations have been used to calculate the external heat loss coefficient at the outside surface of greenhouse covers [39–42]. It depends on the greenhouse geometry under any environmental conditions. Mac Adams [40] suggested a relation, which is used in this study

$$h_{c-o}^C = 5.7 + 3.8 U_o \tag{4}$$

where U_o is the wind speed outside the greenhouse.

The evaluation of internal convective heat transfer coefficient follows Seginer and Livne [42] which considers the combined effect of free and forced convection.

$$h_{c-i}^C = 1.52 |T_c - T_o|^{1/3} + 5.2 \left(\frac{U_{av}}{L_{gh}} \right)^{1/2} \tag{5}$$

$U_{av} = RE/A_v$ is the average speed of the air inside the greenhouse; RE and A_v are the rate of air infiltration and surface area of the vertical section of the greenhouse respectively.

4.2. Energy balance of canopy surface

The energy balance of canopy surface inside the greenhouse is described by the following equation:

$$Q_{ca}^A + Q_{c-ca}^R - Q_{ca}^R - Q_{ca-i}^C - Q_{ca}^L = 0 \tag{6}$$

where Q_{ca}^A is the shortwave radiation absorbed by canopy; Q_{c-ca}^R is the thermal radiations emitted by cover and absorbed by canopy; Q_{ca}^R is the thermal radiation emitted by canopy; Q_{ca-i}^C is the convective heat transfer from canopy to inside air and Q_{ca}^L is the latent heat transfer between the canopy and the inside air of greenhouse.

The energy balance for canopy in the greenhouse Eq. (6) can be written as

$$\tau_c I_T \alpha_{ca} A_{ca} + \varepsilon_c \sigma T_c^4 A_c \alpha_{t,ca} - \varepsilon_{ca} \sigma T_{ca}^4 A_{ca} - h_{ca-i}^C A_{ca} (T_{ca} - T_i) - \frac{d_a C_p LAI}{\gamma} \frac{(P^*(T_{ca}) - P(T_i))}{r_a + r_s} A_{ca} = 0 \tag{7}$$

The evaluation of the convective heat transfer coefficient between the inside air and the canopy, Stanghellini [43] proposed

$$h_{ca-i}^C = \frac{d_a C_p}{1174 {l_{ca}}^{1/2}} (l_{ca} |T_{ca} - T_i| + 207 U_{ca}^2)^{1/4} \tag{8}$$

where U_{ca} is the air velocity through the canopy inside the greenhouse.

$$U_{ca} = U_{av} \left(\frac{l_{ca} A_s}{V_a} \right)^{2/3} \tag{9}$$

The saturated water vapor pressure $P^*(T_{ca})$ at the temperature of the canopy is calculated by Tetens equation (Eq. (10)), the following empirical formula relating accurately saturated water vapor pressure to temperature for the temperature range between 0 and 60 °C [44,45]

$$P^*(T_{ca}) = 0.6108 \exp\left(\frac{17.27 T_{ca}}{T_{ca} + 237.3} \right) \tag{10}$$

The aerodynamic resistance, r_a (sm^{-1}) of the canopy, mainly depends on the aerodynamic regime that prevails in the greenhouse and the leaf length. It is expressed as [45]

$$r_a = 220\frac{l^{0.2}}{U_i^{0.8}} \tag{11}$$

where l is the characteristic length of the leaf and U_i is the mean interior air speeds.

The stomatal resistance r_s (sm^{-1}) of the canopy is derived from a simple empirical relationship, Eq. (12), with global radiation (thermal and humidity dependences of greenhouse plants transpiration were neglected) [45,46]

$$r_s = 200\left(1+\frac{1}{\exp(0.05(\tau_c I_T - 50))}\right) \tag{12}$$

4.3. Energy balance of soil surface

The energy balance of soil surface inside the greenhouse is described by the following equation:

$$Q_s^A - Q_{s-i}^C - Q_s^{Cd} - Q_s^R + Q_{c-s}^R = 0 \tag{13}$$

where Q_s^A is the absorbed solar radiation by soil; Q_{s-i}^C is the convective heat transfer from soil surface to air inside the greenhouse; Q_s^{Cd} is the conductive heat transfer into soil surface; Q_s^R is the thermal heat radiation emitted by soil and Q_{c-s}^R is the thermal heat radiation emitted by greenhouse cover and absorbed by soil.

The energy balance of soil in the greenhouse (Eq. (13)) can be written as

$$I_T\tau_c\alpha_s A_s - h_{s-i}^C A_s(T_s - T_i) - \frac{\lambda_s}{z}A_s(T_s - T_z) - \varepsilon_s\sigma T_s^4 A_s + \varepsilon_c\sigma T_c^4 A_c\alpha_s = 0 \tag{14}$$

The convective heat transfer coefficients between the air inside the greenhouse and soil surface given by Seginer and Livres [42]

$$h_{s-i}^C = 1.52|T_i - T_s| + 5.2\left(\frac{U_{ca}}{L_{gh}}\right)^{1/2} \tag{15}$$

4.4. Energy balance of air inside greenhouse

The energy balance of inside air of greenhouse, only the convective heat transfer is considered. It is assumed that no thermal or solar radiation is absorbed by the air. The energy balance is described by the following equation:

$$Q_{c-i}^C + Q_{ca-i}^C + Q_{s-i}^C - Q_{\inf}^C + Q_H = 0 \tag{16}$$

where Q_{c-i}^C is the convective heat transfer from inside air to cover of the greenhouse, Q_{ca-i}^C is the convective heat transfer from inside air to canopy surface, Q_{s-i}^C is the convective heat transfer from inside air to soil surface, $Q_{\inf}^C$ is the heat loss due to ventilation or infiltration and Q_H is the heat input into greenhouse.

The sensible heat balance of the inside air of greenhouse (Eq. (16)) can be written as

$$h_{c-i}^C A_c(T_c - T_i) + h_{ca-i}^C A_{ca}(T_{ca} - T_i) + h_{s-i}^C A_s(T_s - T_i) - d_a C_p RE(T_i - T_o) + Q_H = 0 \tag{17}$$

where Q_H is the heat gain from the solar air heater with latent storage collector into the IGLHS.

5. Energy balance of the SAHLSC

The energy analysis balance during both the charging and discharging phases of the SAHLSC is

$$Q_A = Q_u + Q_{st} + Q_{los} \tag{18}$$

where Q_A, Q_u, Q_{st}, and Q_{los} are the absorbed, useful, stored and lost energies, respectively.

Based on Duffie and Beckman [47], the useful heat gain from the collector is

$$Q_u = \dot{m}C_p(T_{out} - T_{in}) \tag{19}$$

The radiation absorbed flux of the absorber packed-bed is defined as

$$Q_A = A_p(\alpha_g\tau_g)I_T \tag{20}$$

The stored heat flux during the charging and discharging phases is given by

$$Q_{ch} = [m_{PCM}C_{p,S}(T_m - \overline{T}_{ini_ch,PCM}) + m_{PCM}L + m_{PCM}C_{p,L}(\overline{T}_{fin_ch,PCM} - T_m)]/\Delta t_{ch} \tag{21}$$

$$Q_{dis} = [m_{PCM}C_{p,L}(T_m - \overline{T}_{fin_dis,PCM}) + m_{PCM}L + m_{PCM}C_{p,S}(\overline{T}_{in_dis,PCM} - T_m)]/\Delta t_{dis} \tag{22}$$

The lost heat flux is given by Eq. (23), H_{los} is the collector overall heat loss coefficient. The thermal energy is lost from the collector to the surroundings by conduction, convection and infrared radiation. H_{los} is equal to the sum of energy loss through the top (H_t), bottom (H_b) and edges (H_e) of the collectors given below [47]

$$Q_{los} = H_{los}A_c(\overline{T_P} - T_i) \tag{23}$$

$$H_{los} = H_t + H_b + H_e \tag{24}$$

The top loss coefficient from the collector to the ambient is

$$H_t = (1/(h_{P-g}^C + h_{P-g}^R) + 1/h_{g-a}^R)^{-1} \tag{25}$$

The flow is laminar during the charging phase; and the appropriate correlation is given by Churchill [48]

$$Nu_{ch} = 2 + (0.589\ Ra^{1/4})/(1 + ((0.469)/Pr)^{9/16})^{4/9} \quad \begin{bmatrix} Pr \geq 0.7 \\ Ra \leq 10^{11} \end{bmatrix} \tag{26}$$

Then the flow is turbulent during the discharging phase; the appropriate correlation is given by Whitaker [44]

$$Nu_{dis} = 2 + (0.4\ Re^{1/2} + 0.06\ Re^{2/3})\ Pr^{0.4}(\mu/\mu_s)^{1/4} \quad \begin{bmatrix} 0.71 \leq Pr \leq 380 \\ 3.5 \leq Re \leq 7.6\times 10^4 \\ 1 \leq (\mu/\mu_s) \leq 3.2 \end{bmatrix} \tag{27}$$

$$h_{P-g}^C = Nu(\lambda/t) \tag{28}$$

$$h_{P-g}^R = (\sigma(T_P^2 + T_g^2)(T_P + T_g))/((1/\varepsilon_P) + (1/\varepsilon_g) - 1) \tag{29}$$

$$h_{g-a}^R = \varepsilon_g\sigma(T_g^2 + T_{sky}^2)(T_g + T_{sky}) \tag{30}$$

In addition the energy loss through the bottom (H_b) and the edges (H_e) is as follows:

$$H_b = \lambda_i/\delta_b \tag{31}$$

$$H_e = (L_1 + L_2)L_3\lambda_i/(L_1L_2\delta_e) \tag{32}$$

6. Thermal load leveling (TLL)

The thermal load leveling (TLL) is a relative index to represent the fluctuation of temperature inside the greenhouse. The less the fluctuations, the better is the environment for plants inside the greenhouse. For thermal heating of the greenhouse with minimum

fluctuations the TLL should has a minimum value [49].

$$TLL = \frac{T_{i,\ max} - T_{i,\ min}}{T_{i,\ max} + T_{i,\ min}} \tag{33}$$

7. Results and discussions

7.1. Comparative study of greenhouses climate

In the CG and IGLHS, tomato plants are transplanted on the 23th of January and the harvesting started on the 15th of April 2013. The major environmental factors that affect the growth and the precocity of the production of greenhouse plants are carbon dioxide, light, humidity and temperature. The tomato plants have two optimum temperatures, one during the day; which varied between 20 and 30 °C, and the other nocturnal temperature which is the most crucial temperature, varied between 12 and 18 °C.

During the growing period, the February has the least average monthly radiation is 85 kW/m^2 with a monthly ambient temperature around 12.5 °C (Figs. 2 and 3). An experimental study has been carried out during the month of February 2013 which is the winter season.

Fig. 8 presented the instantaneous registered air temperature inside CG and IGLHS (1st–28th February, 2013). The fluctuation of air temperature inside the two greenhouses is closely attributed to weather conditions such as solar radiation and outside temperature. Under the experimental conditions, the nocturnal variation of temperatures inside greenhouses varied between 2 and 5 °C. The method of utilizing the new solar air heater with latent storage collector as a heating system inside the greenhouse shows meaningful value in February.

An experimental study has been carried out on typical selected days of the system operation from 23th to 27th February, 2013 in winter season.

The external global solar radiation and wind speed for the 5-day period in the region of the greenhouses are shown in Fig. 9. The maximum of the global solar irradiation intensity in the horizontal plane varied between 300 and 650 Wm^{-2}. The two first days of this period were very windy, air speed varied between 3 and 8 ms^{-1}. The average speed of other days is of 2 ms^{-1}.

The daily variation of the ambient temperature, air temperature inside CG and air temperature inside IGLHS are presented in Fig. 10 (for the same 5-day period). The air temperature inside the greenhouses followed the same trend as the ambient temperature and exceeds the daily tomato optimum temperature under severe winter weather. Consequently, it is necessary to improve the air conditioning of this greenhouse. A new solar air heater collector with a latent heat storage system is integrated inside the IGLHS. This collector is used to store the excess of the transmitted solar irradiation in the packed bed absorber and to provide it at night. The discharging process of the SAHLSC starts at 21 h (local time). A fan was used to blow the air at a fixed speed equal to 1m/s.

The 23th and 27th of February, 2013 is characterized by clear sky with maximum ambient temperature equal to 21 °C. We observed that the diurnal temperature attained 39 °C and 41 °C respectively into CG and into IGLHS. The nocturnal variation of temperature inside the IGLHS exceeds the temperature inside CG with a difference of 5 °C from 21 h (local time) until the morning after (Fig. 10). On 27th of February, 2013 the SAHLSC maintained the air temperature inside IGLHS constant, around 12 °C, along the night, due to the fraction of solar radiations stored in the packed bed absorber. However, the temperature inside CG decreases progressively to the ambient temperature after 2 h from sunset. The 24th February, 2013 was characterized by severe solar radiation fluctuations, the ambient air temperature does not exceed 11 °C and wind velocity varied from 4 to 8 m/s. We noted that the

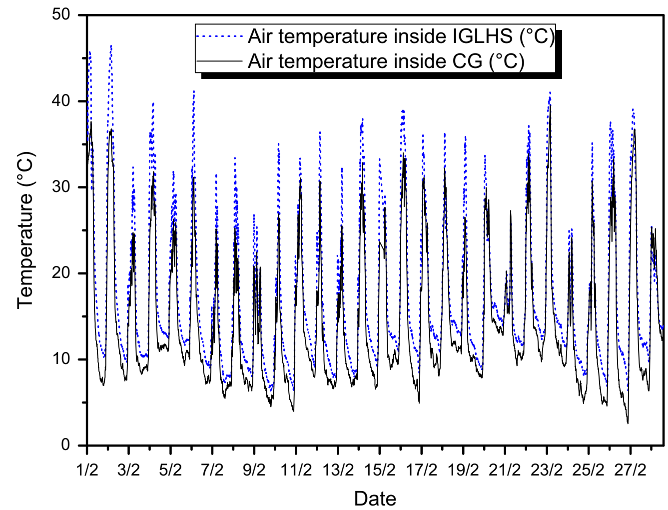


Fig. 8. Air temperature inside CG and air temperature inside IGLHS as a function of days. (1st–28th February, 2013).

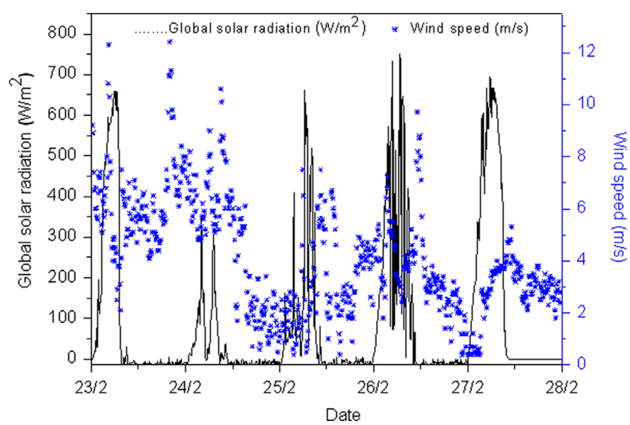


Fig. 9. Global solar radiation and wind velocity as a function of days (23th–27th February, 2013).

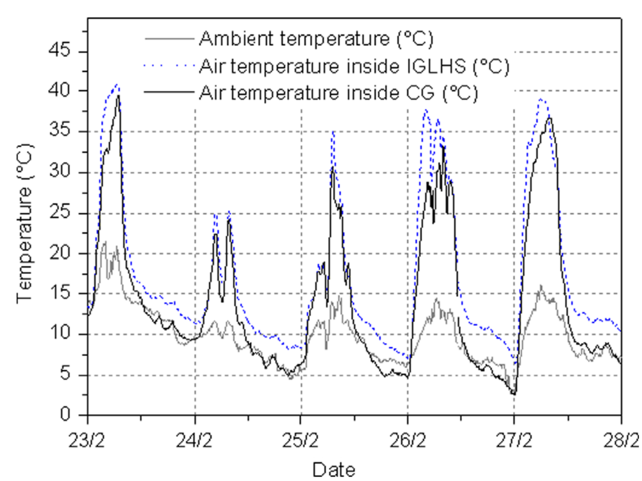


Fig. 10. Ambient temperature, air temperature inside CG and air temperature inside IGLHS as a function of days (23th–27th February, 2013).

temperature into the IGLHS exceeds the temperature inside CG with a difference of 3 °C all the night.

Fig. 11 presents the effect of the SAHLSC on relative humidity inside the greenhouse. At night, the IGLHS permitted to maintain the air relative humidity to 10–20% lower than the CG. The SAHLSC

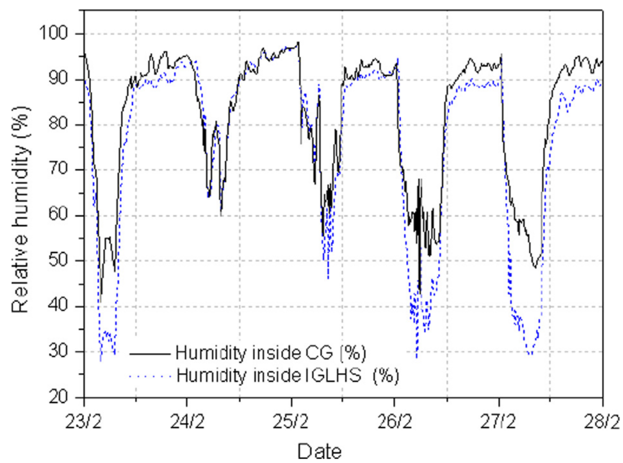


Fig. 11. Humidity inside CG and IGLHS as a function of days (26th–27th February, 2013).

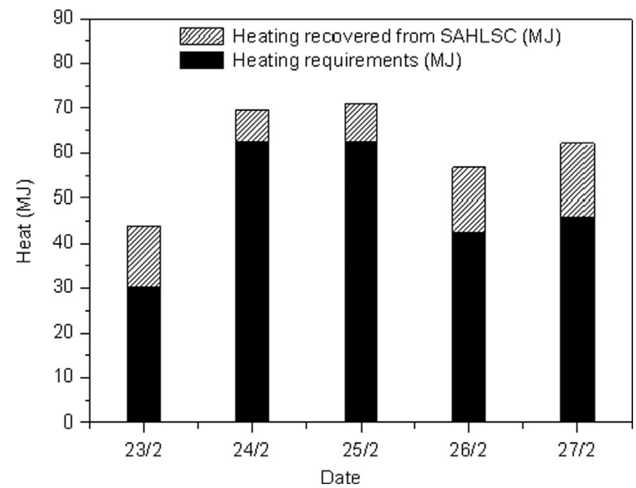


Fig. 13. Nighttime heating recovered from SAHLSC and IGLHS heating requirements as a function of days (26th–27th February, 2013).

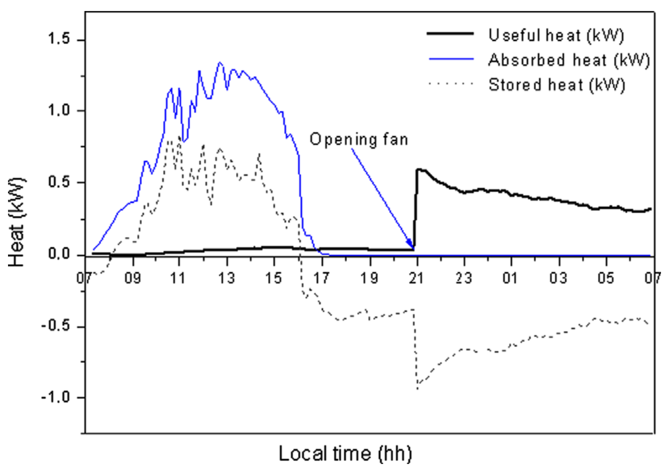


Fig. 12. Useful, absorbed and stored heat rates as a function of day times inside the IGLHS (27th February, 2013).

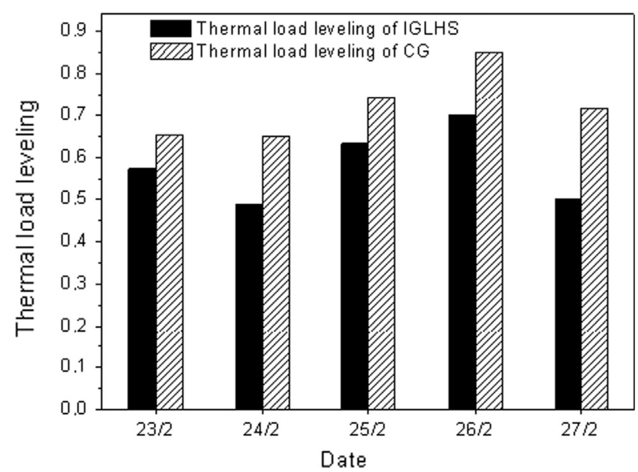


Fig. 14. Thermal load leveling of CG and IGLHS as a function of days (26th–27th February, 2013).

creates a passive dehumidification process at night time due to the increase of the air temperature inside the IGLHS.

7.2. Performance of the SAHLSC inside IGLHS

Variations of useful, absorbed and stored energy are presented in Fig. 12 during 27th of February, 2013. Therefore, to evaluate the stored energy, the energy balance equation (Eq. (18)) has been used. A great part of the absorbed solar heat was stored inside the PCM. It is observed that during the initial period of charging, the instantaneous heat stored increases with insolation and towards a maximum value of 0.7 kW at 13:00, we noted that at this time the absorbed heat is 1.3 kW, 53% of the solar energy is stored into the collector. As the discharging process proceeds, the PCM starts solidifying and the used heat is uniform for a longer period. The uniform value of the used heat is between 550 and 300 W all the night.

Energy balance equation (Eqs. (2), (6), (13), (17) and (18)) have been used for calculating requirements, excess and recovered thermal energy (MJ) inside IGLHS. Fig. 13 presented the daily heating requirements and the nighttime heating recovered from SAHLSC, during the 5-days period (23th–27th February, 2013). The stored energy in the solar air heater with thermal storage is 13.7 MJ on 23th February, 2013. The contribution of stored energy in the SAHLSC to the nighttime heating requirements was 31%, 27% and 26% respectively on 23th, 26th and 27th February, 2013 under best ambient conditions. On 24th and 25th February, 2013, the recovered and stored heat is 6% and 11% with requirements heat exceeds 65 MJ.

The performance of IGLHS with a SAHLSC heating system has been evaluated in terms of thermal load leveling, TLL, using Eq. (3). The TLL is used to quantify the fluctuations of temperature inside the greenhouse. In winter, TLL should have lower value by incorporating a heating system due to the increase of $(T_{i,\,max}+T_{i,\,min})$ as well as decrease of $(T_{i,\,max}-T_{i,\,min})$ as compared to TLL without heating system. The results of the daily variation of thermal load leveling for CG and IGLHS greenhouse have been shown in Fig. 14. It can be seen that the value of TLL is maximum for CG greenhouse and it is reduced to 25% for IGLHS on 27th February, 2013. The lower values of thermal load leveling indicate the decrease in the fluctuations of greenhouse air and thereby, there occurs an improvement of desired environment for plants in the greenhouse.

8. Economic analysis

The economic analysis (SAHLSC cost, energy cost and payback period in comparison with the expected service life cycle of the installation) is done without taking into account the interest and the inflation, we suppose that all the cost is paid without credit payment [50]. The life cycle of the SAHLSC is considered 20 years

and its thermal performance degradation is assumed to be 1% per year.

In order to evaluate the economic analysis, the SAHLSC system is compared to non-solar alternative heating system (fuel boiler). In this study, two systems are considered:

- Hybrid system: the SAHLSC and the fuel boiler. The fuel boiler is the auxiliary system meeting the energy needs.
- Conventional system: the most heating system used for greenhouses conditioning is the fuel boiler.

8.1. The total cost system

The total cost of the greenhouse heating system includes the investment cost and the energy consumption cost. The investment cost includes the system cost and the operation and maintenance cost [51,52].

The total cost of the conventional system is defined by adding the initial investment cost of the fuel boiler and the fuel consumption. For the hybrid system the total cost is the sum of all the initial investment cost (SAHLSC+fuel boiler) and the fuel consumption without the supplied heat cost by the SAHLSC.

- The system cost is defined by the equipment, the realization and the installation costs. The hybrid system cost includes the fuel boiler and SAHLSC costs. Since the SAHLSC is not yet commercialized, there is no official price for this system. Thus, the capital cost of the solar collector was roughly determined as the costs spent to develop the experimental system.
- The operation and maintenance cost refers to heat production coupled with full load hours. The electricity consumption for operating the fan was considered as operating costs. The maintenance cost of the SAHLSC is considered negligible.

8.2. Energy consumption for the greenhouse heating

The sizing of the greenhouse heating system is based on the nocturnal setpoint temperature (12 °C). This temperature is suitable for tomato cultivation implemented in the experimental greenhouse. The necessities of the energy to maintain the nocturnal air temperature under the greenhouse at the setpoint value is equal to the energy losses. The total energy losses are determined by adding the energy losses of the greenhouse components (cover, ground, infiltration, and canopy). The Tunisian greenhouse heating period is from November to March, equivalent to 1500 h of heating. In this period, the fuel boiler in the hybrid system, functions only 600 h. Therefore it ensures an economy of 1800 kWh/year.

8.3. The payback duration

The aim of the economical analysis is to find out the payback period of the SAHLSC. The payback duration indicates the time that the SAHLSC generates the amount of energy equivalent to the energy provided during the life cycle [53].

The cost of each heating systems (hybrid and conventional system) and the payback time of the SHALSC is mentioned in Table 2. As a result, the payback period of solar air heater with latent storage is found as 5 years.

8.4. Environmental impact of the SAHLSC

From 2005 to 2008, the greenhouse areas of Tunisia increased from 4600 ha to 9000 ha [54], which consume 3×10^5 t of fuel during 5 months of heating period. The maximum of the CO_2 content is about 16% of the fuel consumption [55], therefore the conventional heating system causes the emission of 3.12×10^5 t of CO_2 which is equal to 2.8×10^{-2} t per person [56]. The reduction of carbon dioxide emissions using the SAHLSC may be a promising solution. Indeed, the SAHLSC ensure the greenhouse conditioning during 3 months, it can reduce the CO_2 emission at 1.68×10^{-2} t per person which presents 1% of the total of the CO_2 emissions.

Table 2
Comparison of the cost and the payback times between SAHLSC system and the fuel boiler.

	Hybrid system (SAHLSC+fuel boiler)	Conventional system (fuel boiler)
System cost ($)	3600	1800
Operation cost ($)	4.75	116.55
Maintenance cost ($)	150	150
Annual energy consumption (kWh)	1200	3000
Gain of energy (kWh)	1800	–
Energy cost ($)	259.2	651.25
Total cost	4014	2717.8
Payback of SAHLSC (year)	5	–

9. Conclusion

An experimental study was conducted to evaluate the nighttime recovered heat of the SAHLSC in the east–west oriented greenhouse. During winter months, the maximum of solar radiation falls on the south wall. Therefore, a SAHLSC is proposed in this study for storing the excess of the transmitted solar irradiation in the packed bed absorber and to provide it at night. This stored energy is extracted to the greenhouse by convection and radiation heat. The performance of the solar system was evaluated in terms of thermal load leveling and nighttime recovered heating for a 5-day period of February, 2013 in Tunisia. As a result of this system, the amount of the nighttime recovered heat of this system attains 31% of the total requirements of heating. The relative humidity was found to be an average 10–20% lower at night time inside the heated greenhouse. The nocturnal variation of temperature inside the IGLHS exceeds the temperature inside the CG by 5 °C. The solar air heater remains a uniform useful heat during the nighttime. The uniform value of the used heat is between 550 and 300 W all the night. This useful heat was not affected by the severe global solar radiation fluctuation during the charging mode. The evaluation of the economic analysis of the SAHLSC assessed that the payback period was approximately 5 years if the system operates only 3 months per year. The environmental impact from reducing carbon emissions is about 1% of the total Tunisian greenhouses emissions.

Acknowledgments

This study was supported by the Thermal Processes Laboratory of the Research and Technology Center of Energy (CRTEn) in Tunisia.

References

[1] Von Elsner B, Briassoulis D, Waaijenberg D, Mistriotis A, von Zabeltitz C, Gratraud J, et al. Review of structural and functional characteristics of greenhouses in the European Union countries: Part I, design requirements. J Agric Eng Res 2000;75:1–16.

[2] Max JFJ, Horst WJ, Mutwiwa UN, Tantau HJ. Effects of greenhouse cooling method on growth, fruit yield and quality of tomato (*Solanum lycopersicum* L.) in a tropical climate. Sci Hortic 2009;122:179–86.
[3] Briassoulis D, Waaijenberg D, Gratraud J, Von Elsner B. Mechanical properties of covering materials for greenhouses: Part 1, general overview. J Agric Eng Res 1997;67:81–96.
[4] Yang SH, Rhee JY. Utilization and performance evaluation of a surplus air heat pump system for greenhouse cooling and heating. Appl Energy 2013;105: 244–51.
[5] Berroug F, Lakhala EK, El Omaria M, Faraji M, El Qarnia H. Thermal performance of a greenhouse with a phase change material north wall. Energy Build 2011;43:3027–35.
[6] Panwar NL, Kaushik SC, Kothari S. Solar greenhouse an option for renewable and sustainable farming. Renew Sustain Energy Rev 2011;15:34–45.
[7] Garcia JL, De la Plaza S, Navas LM, Benevente RM, Luna L. Evaluation of the feasibility of alternative energy sources for greenhouse heating. J Agric Eng Res 1998;69:107–14.
[8] Sethi VP, Sharma SK. Survey and evaluation of heating technologies for worldwide agricultural greenhouse applications. Sol Energy 2008;82:832–59.
[9] Barral JR, Galimberti PD, Barone A, Miguel AL. Integrated thermal improvements for greenhouse cultivation in the central part of Argentina. Sol Energy 1999;67:111–8.
[10] Bargach MN, Tadili R, Dahman AS, Boukallouch M. Survey of agricultural greenhouses in Morocco. Renew Energy 2000;20:415–33.
[11] Santamouris M, Mihalakakou G, Balaras CA, Lewis JO, Vallindras M, Argirious A. Energy conservation in greenhouses with buried pipes. Energy 1996;21:353–60.
[12] Du J, Bansal P, Huang B. Simulation model of a greenhouse with a heat-pipe heating system. Appl Energy 2012;93:268–76.
[13] Hasnain SM. Review on sustainable thermal energy storage technologies Part 1: heat storage materials and techniques. Energy Convers Manag 1998;39: 1127–38.
[14] Farid MM, Khudhair AM, Razack SAK, Al-Hallaj S. A review on phase change energy storage: materials and applications. Energy Convers Manag 2004;45:1597–615.
[15] Dincer I, Rosen MA. Thermal energy storage: system and applications. John Wiley and Sons, New York, USA; 2006.
[16] Zhou D, Zhao CY, Tian Y. Review on thermal energy storage with phase change materials (PCMs) in building applications. Appl Energy 2012;92:593–605.
[17] Tian Y, Zhao CY. A review of solar collectors and thermal energy storage in solar thermal applications. Appl Energy 2013;104:538–53.
[18] Lazaar M, Kool S, Hazami M, Farhat A, Belghith A. Use of solar energy for the agricultural greenhouses autonomous conditioning. Desalination 2004;168:169–75.
[19] Bouhdjar A, Belhamel M, Belkhiri FE, Boulbina A. Performance of sensible heat storage in a rock bed used in a tunnel greenhouse. Renew Energy 1996;9:724–8.
[20] Willits DH, Chandra P, Peet MM. Modeling solar energy collection/storage system for greenhouses. J Agric Eng Res 1985;32:73–9.
[21] Bakos GC, Fidanidis D, Tsagas NF. Greenhouse heating using geothermal energy. Geothermics 1999;28:759–65.
[22] Adaro JA, Galimberti PD, Lema AI, Fasulo A, Jorge R, Barral JR. Geothermal contribution to greenhouse heating. Appl Energy 1999;64:241–9.
[23] Vadiee A, Martin V. Thermal energy storage strategies for effective closed greenhouse design. Appl Energy 2013;109:337–43.
[24] Benli H, Durmuş A. Performance analysis of a latent heat storage system with phase change material for new designed solar collectors in greenhouse heating. Sol Energy 2009;83:2109–19.
[25] Huang BK, Toksoy M, Cengel YA. Transient response of latent heat storage in greenhouse solar system. Sol Energy 1986;37:279–92.
[26] Alkilani MM, Sopian K, Alghoul MA, Sohif M, Ruslan MH. Review of solar air collectors with thermal storage units. Renew Sustain Energy Rev 2011;15: 1476–90.
[27] Sharma A, Tyagi VV, Chen CR, Buddhi D. Review on thermal energy storage with phase change materials and applications. Renew Sustain Energy Rev 2009;13:318–45.
[28] Kern M, Aldrich RA. Phase change energy storage in a greenhouse solar heating system. ASME paper no. 79-4028. St. Joseph, MI: Am. Soc. Agric. Eng.;1979.
[29] Huang K, Toksoy M. Design and analysis of greenhouse solar system in agricultural production. Energy Agric 1983;2:115–36.
[30] Levav N, Zamir N. Phase change materials for heat storage in greenhouse. REUR technical series L: greenhouse heating with solar energy. CNRE; 1987. p. 163–166.
[31] Boulard T, Baille J. Thermal performance and model of two types of greenhouses with solar energy storage. Acta Hortic 1987;263:121–30.
[32] Boulard T, Razafinjohany E, Baille A, Jaffrin A, Fabre B. Performance of a greenhouse heating system with a phase change material. Agric Fo Meteorol 1990;52:303–18.
[33] Öztürk HH. Experimental evaluation of energy and exergy efficiency of a seasonal latent heat storage system for greenhouse heating. Energy Convers Manag 2005;46:1523–42.
[34] National Renewable Energy Laboratory (NREL). 〈http://www.nrel.gov/gis/images/swera/africa/africa_tilt.jpg〉.
[35] Nation Institute of Metrological of Tunisia. 〈http://www.meteo.tn〉.
[36] Bouadila S, Kooli S, Lazaar M, Skouri S, Farhat A. Performance of a new solar air heater with packed-bed latent storage energy for nocturnal use. Appl Energy 2013;110:267–75.
[37] 〈http://www.campbellsci.com〉.
[38] Manwell JF, McGowan JG, Rogers AL. Wind energy explained: theory, design and application. 2nd ed.. New York, USA: John Wiley and Sons; 2009.
[39] Papadakis G, Frangoudakis A, Kyritsis S. Mixed forced and free convection heat transfer at the greenhouse cover. J Agric Eng Res 1992;51:191–205.
[40] Mac Adams WH. Heat transmission. third ed.Mac Graw-Hill, New York, USA; 1954.
[41] Kindelan M. Dynamic modeling of greenhouse environment. Trans ASAE 1980:1232–9.
[42] Seginer I., Livne A. Effect of ceiling height on the power requirement of forced ventilation in greenhouses: a computational study. IBM Israel Scientific Center; 1978.
[43] Stanghellini C. Transpiration of greenhouse crops, an aid to climate management (Ph.D. dissertation). Netherlands: Wageningen Agricultural University; 1987.
[44] Tetens VO. Uber einige meteorologische. Begr Z Geophys 1930;6:297–309.
[45] Boulard T, Wang S. Greenhouse crop transpiration simulation from external climate conditions. Agric For Meteorol 2000;100:25–34.
[46] Boulard T, Mermier M, Fargues J, Smits N, Rougier M, Roy JC. Tomato leaf boundary layer climate: implications for microbiological whitefly control in greenhouses. Agric For Meteorol 2002;110:159–76.
[47] Duffie JA, Beckman WA. Solar engineering of thermal processes. 2nd ed.. New York, USA: John Wiley and Sons; 1991.
[48] Incropera FP, DeWitt DP, Bergman TL, Lavine AS. Fundamentals of heat and mass transfer. 6th ed.. New York: USA: John Wiley and Sons; 2007.
[49] Sutar RF, Tiwari GN. Analytical and numerical study of a controlled-environment agricultural system for hot and dry climatic conditions. Energy Build 1995;23:9–18.
[50] Kalogirou S. Thermal performance, economic and environmental life cycle analysis of thermo siphon solar water heaters. Sol Energy 2009;83:39–48.
[51] Al-Salaymeh A, Al-Rawabeh I, Emran S. Economical investigation of an in integrated boiler–solar energy saving system in Jordan. Energy Convers Manag 2010;51:1621–8.
[52] Raugei M, Bargigli S, Ulgiati S. Life cycle assessment and energy pay-back time of advanced photovoltaic modules: CdTe and CIS compared to poly-Si. Energy 2007;32:1310–8.
[53] Ardente F, Beccali G, Cellura M, Brano VL. Life cycle assessment of a solar thermal collector. Renew Energy 2005;30:1031–54.
[54] Agency of Agricultural Investments Promotion. Les cultures maraichères sous abris. www.apia.com.tn/pdf/abri.pdf.
[55] Techniques Des Brûleurs A Mazout, No. 301 6ème Edition, La Société Des Equipements Charmilles-Cuenod Annemasse, 2001 (Handbook: technique of oil burners, 6th ed.).
[56] Ramakrishna R. An analysis of energy consumption and carbon dioxide emission in countries of the Middle East and North Africa. Energy 2005;30: 2831–42.